

# Corrosion resistance and antithrombogenic behavior of La and Nd ion implanted stainless steels

F. J. Jing

Department of Physics and Materials Science, City University of Hong Kong, Tat Chee Avenue, Kowloon, Hong Kong, China and College of Materials Science and Engineering, Southwest Jiaotong University, Chengdu 610031, China

F. Y. Jin

Department of Physics and Materials Science, City University of Hong Kong, Tat Chee Avenue, Kowloon, Hong Kong, China and Southwestern Institute of Physics, Chengdu 610041, China

Y. W. Liu and G. J. Wan

College of Materials Science and Engineering, Southwest Jiaotong University, Chengdu 610031, China

X. M. Liu, X. B. Zhao, and R. K. Y. Fu

Department of Physics and Materials Science, City University of Hong Kong, Tat Chee Avenue, Kowloon, Hong Kong, China

Y. X. Leng and N. Huang

College of Materials Science and Engineering, Southwest Jiaotong University, Chengdu 610031, China

Paul K. Chu<sup>a)</sup>

Department of Physics and Materials Science, City University of Hong Kong, Tat Chee Avenue, Kowloon, Hong Kong, China

(Received 21 April 2006; accepted 9 June 2006; published 3 August 2006)

Lanthanide ions such as lanthanum (La) and neodymium (Nd) were implanted into 316 stainless steel samples using metal vapor vacuum arc to improve the surface corrosion resistance and antithrombogenic properties. X-ray photoelectron spectroscopy shows that lanthanum and neodymium exist in the +3 oxidation state in the surface layer. The corrosion properties of the implanted and untreated control samples were investigated utilizing electrochemical tests and our results show that La and Nd implantations enhance the surface corrosion resistance. *In vitro* activated partial thromboplastin time (APTT) tests were used to evaluate the antithrombogenic properties. The APTT time of the implanted samples was observed to be prolonged compared to that of the unimplanted stainless steel control. La and Nd ion implantations can be used to improve the surface corrosion resistance and biomedical properties of 316 stainless steels. © 2006 American Vacuum Society. [DOI: 10.1116/1.2219758]

## I. INTRODUCTION

Rare earth elements have aroused considerable interests in the field of medicine due to their special pharmacological effects. With relatively low toxicity, rare earth elements exhibit anticoagulant, antiemetic, antiseptic, immunomodulatory, and antineoplastic properties.<sup>1-3</sup> Lanthanide elements are very reactive with oxygen and they can play an important role in the improvement of the corrosion resistance of materials.<sup>4-8</sup> Lanthanides can be incorporated into metals using different methods such as simple alloying, chemical baths, and ion implantation. In particular, ion implantation has been shown to be very useful in modifying the surface chemical behavior of materials. The use of ion implantation to improve the corrosion performance of materials has been reported.<sup>9-16</sup> In the work described here, lanthanide ions such as lanthanum and neodymium were implanted into 316 stainless steels which are commonly used in orthopedic implants. The corrosion properties of the treated samples in simulated

body fluids (SBFs) were investigated using electrochemical tests and the antithrombic properties performance of the samples were evaluated by *in vitro* activated partial thromboplastin time (APTT) tests.

## II. EXPERIMENTAL DETAILS

The compositions (at. %) of 316 stainless steel samples are as follows: Cr: 17.0–19.0, Ni: 11.0–13.0, Mo: 1.5–2.5, Mn: ≤0.6, Si: <1.0, C: 0.06, O: <0.16, Fe: balance. The specimens ( $1 \times 1 \times 0.2$  cm<sup>3</sup>) were mechanically ground to a shiny finish and then ultrasonically cleaned in acetone and ethanol before ion implantation. Implantations of Nd and La were conducted using a metal vapor vacuum vapor arc (MEEVA) source at 40 kV at a working pressure of  $2 \times 10^{-3}$  Pa. The implant fluence is about  $1.0 \times 10^{17}$  ions cm<sup>-2</sup>.

The elemental depth profiles and surface chemical composition of the implanted samples were determined by x-ray photoelectron spectroscopy (XPS) by the  $K_{\alpha}$  line of the Al x-ray source using a Physical Electronics PHI 5802 Auger/XPS instrument. The samples were sputtered by an Ar

<sup>a)</sup>Author to whom correspondence should be addressed; electronic mail: paul.chu@cityu.edu.hk

ion beam at a sputtering rate of 4.7 nm/min calibrated using SiO<sub>2</sub> under similar conditions. Electrochemical tests based on the ASTM G5-94 (1999) and G61-86 (1998) protocols were conducted to evaluate the surface corrosion resistance of the samples. The tests were conducted in SBFs at a pH value of 7.42 and temperature of 37 °C. The scanning rate was 600 mV/h. After the corrosion tests, the surface morphology was studied by scanning electron microscopy (SEM).

The activated partial thromboplastin time (APTT) is commonly used clinically to detect abnormality in blood plasma and screen anticoagulative chemicals.<sup>17</sup> In our experiments, the samples were attached to a silanizing tube with fresh human platelet-poor blood plasma and incubated at 37 °C for 15 min. The samples were taken out immediately and an incubating solution with actin-activated cephaloplastin reagent was added to the test tubes and incubated at 37 °C for 3 min. Following the addition of a 0.03M CaCl<sub>2</sub> solution, the clotting time was measured by a coagulometer.

### III. RESULTS AND DISCUSSION

#### A. Composition and depth profiles

XPS measurements were carried out to determine the concentration of the elements in the surface as a function of depth. Figures 1(a) and 1(b) show the results acquired from the La and Nd ion implanted stainless steel samples, respectively. It can be observed that the implanted depths of La and Nd are 40 and 50 nm, respectively. It should be noted that these profiles have been plotted on a depth scale based on a sputtering rate calculated from a SiO<sub>2</sub> reference under similar conditions. Since it is well known that the sputtering rate changes in the surface region and is different from that of SiO<sub>2</sub>, the thicknesses of the implanted layers shown here are only approximate, although comparison among the samples is more valid. A fairly large amount of surface oxygen is also detected and it will be discussed later.

High-resolution XPS spectra were taken at different sputtered depths to investigate the chemical states of the implanted species. Figure 2 displays the La3d and O1s montage spectra at different sputtering times. The La3d spectrum in Fig. 2(a) shows two doublets in the 3d<sub>5/2</sub> and 3d<sub>3/2</sub> peaks and the energy difference between the 3d<sub>3/2</sub> and 3d<sub>5/2</sub> levels is approximately 17 eV. The La3d states split into two lines 3d<sub>5/2</sub> and 3d<sub>3/2</sub> because of a spin-orbit interaction. The O1s intensity decreases with increasing sputtering time. The energy peaks appearing on the high energy side of the 3d<sub>5/2</sub> and 3d<sub>3/2</sub> peaks after sputtering for 0, 1, 2, and 3 min are the satellite peaks. The split of the 3d<sub>5/2</sub> and 3d<sub>3/2</sub> peaks is due to a transfer of an electron from O2p to the empty 4f shell of La leading to the 3d<sup>9</sup>4f<sup>1</sup> final state.<sup>18</sup> The La3d line has a main line *M* (ascribed to 3d<sup>9</sup>4f<sup>0</sup>) and a satellite line *S* (ascribed to a charge transfer 3d<sup>9</sup>4f<sup>1</sup>*L* where *L* represents the hole in a ligand site) at higher binding energy. Oxygen uptake is also evident from the splitting of the La3d peak upon oxygen exposure.

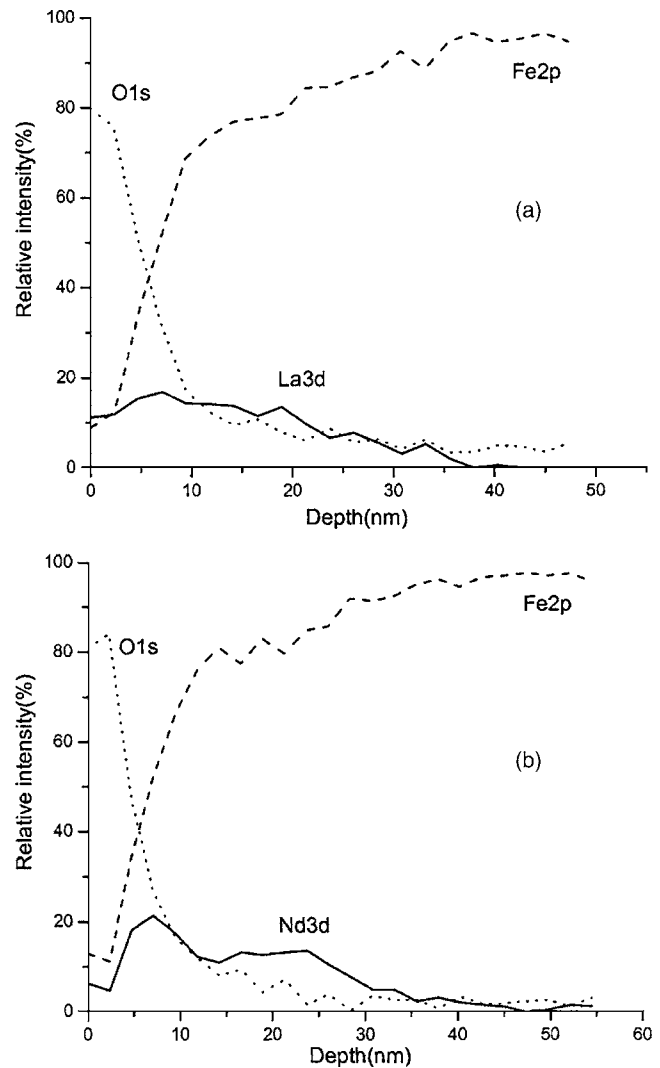


Fig. 1. XPS depth profiles: (a) La implanted SS and (b) Nd implanted SS.

The La3d<sub>5/2</sub> peak of the as-implanted surface is at approximately 835.1 eV, which according to the literature,<sup>19</sup> corresponds to aged (hydrated) La<sub>2</sub>O<sub>3</sub>. The binding energy of the oxygen peak (~532 eV) suggests a strong contribution from hydroxide species and the energy peak lower by about 1.8 eV corresponds to the O<sup>2-</sup> ion of the sesquioxide on the as-implanted surface. These results show that hydrated La<sub>2</sub>O<sub>3</sub> exists on the as-implanted surfaces after exposure to air. After sputtering for 1, 2, and 3 min, the La3d<sub>5/2</sub> core sputtering level exhibits a 0.8–1.0 eV shift towards a lower binding energy compared to the as-implanted surface. The corresponding binding energy of La3d<sub>5/2</sub> is about 834.4 eV. The binding energies and the multiplet splitting agree well with reported values for lanthanum in the +3 oxidation state.<sup>20–24</sup> The O1s state also shows a clear simultaneous change. The most intense peak at a binding energy of 530 eV corresponds to O<sup>2-</sup> of the sesquioxide. Therefore, the La XPS profiles acquired after sputtering for 1, 2, and 3 min reveal oxides of lanthanum species such as La<sub>2</sub>O<sub>3</sub>. After sputtering for 4 min, the single peak initially observed at

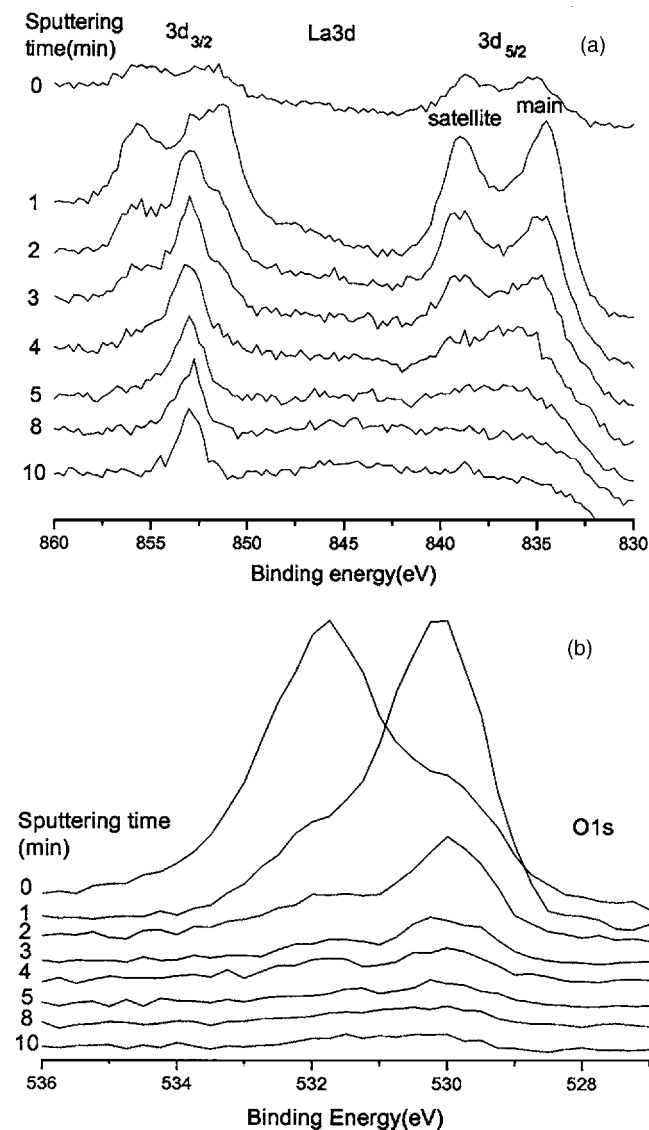


FIG. 2. High-resolution XPS spectra obtained at different sputtering times from the La implanted stainless steel sample: (a) La3d and (b) O1s.

836.4 eV in the La3d spectrum and the O1s peak decrease significantly, as shown in Fig. 2. This is due to the emergence of metallic La.

Figure 3 shows the Nd3d and O1s high-resolution XPS spectra at different sputtering times. The Nd3d spectrum in Fig. 3(a) shows two doublets of 3d<sub>5/2</sub> and 3d<sub>3/2</sub> and the energy difference between the 3d<sub>3/2</sub> and 3d<sub>5/2</sub> levels is approximately 22.6 eV. The peak around 981.0–982.0 eV is indicative of Nd<sub>2</sub>O<sub>3</sub>,<sup>25</sup> and the satellite peaks after sputtering for 1 and 2 min are on the lower energy side of the main peak. The Nd3d spectra show satellite lines related to electron transfer from the oxygen ligand to Nd4f.<sup>26,27</sup> Similar to the peak of O1s of stainless steel (SS) implanted with La, the O1s peak observed at the Nd implanted surface at a binding energy of 530 eV corresponds to O<sup>2-</sup> of the sesquioxide. The peak at a higher energy of 1.8 eV is associated with surface hydroxide or carbonate species. The satellite of the Nd3d line diminishes with increasing sputtering time, probably due to a small

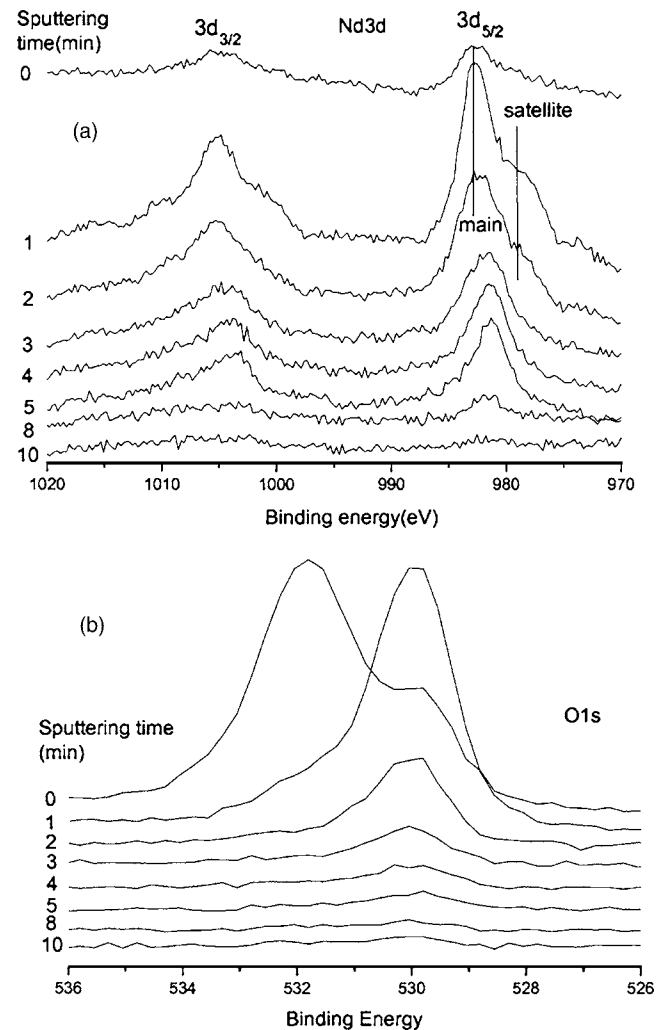


FIG. 3. High-resolution XPS spectra obtained at different sputtering times from the Nd implanted stainless steel sample: (a) Nd3d and (b) O1s.

amount of oxygen. After sputtering for 3, 4, 5, 8, and 10 min, the single peak observed in the Nd3d spectra shows metallic Nd.

Our results show that the stainless steel samples implanted with La and Nd contain La<sub>2</sub>O<sub>3</sub> and Nd<sub>2</sub>O<sub>3</sub> oxides from the surface to about 10–20 nm deep. At larger depths, metallic La and Nd are the dominant species.

## B. Corrosion behavior of La and Nd implanted stainless steel

Figure 4 shows the potentiodynamic polarization curves acquired from the unimplanted as well as the La and Nd implanted samples. The corrosion current densities ( $I_{\text{corr}}$ ) of the La and Nd implanted samples are about one order of magnitude smaller than that of the SS control sample. In addition, the implanted samples exhibit remarkable corrosion resistance in the anodic scanning area compared to SS, as evidenced by the passive current density [ $\log(\text{A}/\text{cm}^2)$ ] changing from  $-4.64$  (SS) to  $-6.61$  (implanted with La) and  $-6.59$  (implanted with Nd). The corrosion potential ( $E_{\text{corr}}$ ) tends to be more negative after La and Nd implantations, and

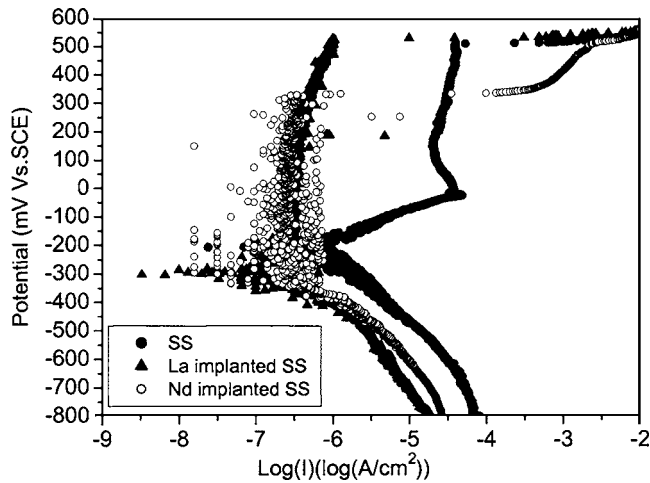


FIG. 4. Corrosion curves acquired from electrochemical tests in cyclic potential mode in SBF from SS and SS implanted with La or Nd.

the negative shift of  $E_{\text{corr}}$  indicates more unstable states that can degrade more rapidly. Nevertheless,  $E_{\text{corr}}$  shows just one aspect of the thermodynamics, and it is not always true that a negative  $E_{\text{corr}}$  correlates to a higher corrosion current density, because it depends on both the thermodynamic and kinetic aspects of the corrosion reactions.<sup>28</sup> The pitting potential is 511 mV for SS, 530 mV for SS implanted with La, and 331 mV for SS implanted with Nd. Figure 5 exhibits the surface morphologies of samples after the electrochemical tests. The pits on the surface of the SS control are bigger and have irregular shape. Some of them are also very deep. In contrast, the pits on the La and Nd implanted samples are smaller and shallower.

It can thus be concluded that La and Nd implantations enhance the corrosion resistance of 316L SS by reducing the formation and growth of corrosion pits. According to the XPS results, the implanted lanthanum and neodymium exist in the forms of  $\text{La}_2\text{O}_3$  and  $\text{Nd}_2\text{O}_3$  in the surface layer. They serve as barrier layers that effectively impede the penetration of the solution ions.

### C. APTT of SS implanted with La and Nd

The APTT reveals the bioactivity of the intrinsic blood coagulation factors and can be used to evaluate the antithrombogenicity of biomaterials *in vitro*.<sup>29,30</sup> Figure 6 shows that the activated partial thromboplastin time of the La and Nd implanted samples is prolonged, indicating that activation of the intrinsic blood coagulation system is suppressed after La and Nd implantations. It has been reported that the thromboplastin-induced clotting time in the presence of 0.5 mM of rare earth metals can be prolonged by a factor of 2.7–14.8.<sup>31</sup> Lanthanide ions ( $\text{Ln}^{3+}$ ) and  $\text{Ca}^{2+}$  ions are remarkably similar in their size, bonding, coordination geometry, and donor atom preference.<sup>32</sup> Lanthanide ions can bind stoichiometrically to the metal binding sites of proteins such as factor X and thrombin more tightly than  $\text{Ca}^{2+}$ .<sup>33</sup> Calcium ions ( $\text{Ca}^{2+}$ ) are also crucial to the blood coagulation cascade and fibrin formation in the intrinsic and extrinsic pathways.<sup>34</sup>

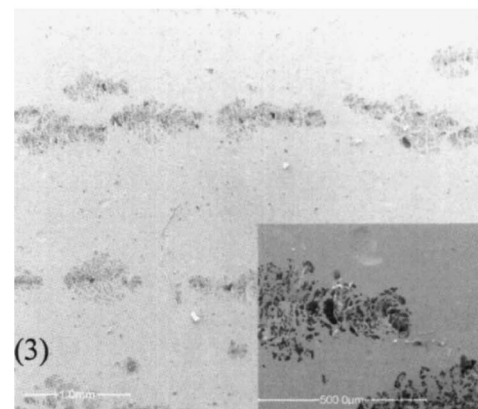
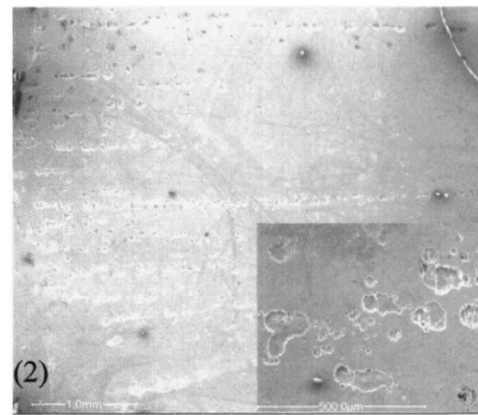
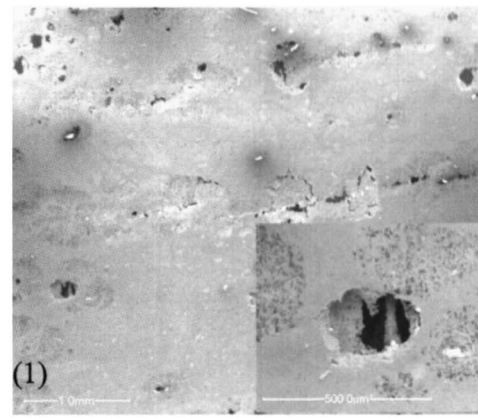


FIG. 5. SEM images after electrochemical tests (30 $\times$  and 100 $\times$ ): (1) SS, (2) SS implanted with La, and (3) SS implanted with Nd.

Prothrombin, a plasma zymogen with a molecular weight of 70 000, is involved in the final stages of blood coagulation.<sup>35</sup> Factor X can convert prothrombin to thrombin, and thrombin can convert fibrinogen to fibrin activating factor XIII, leading to thrombosis. Consequently, lanthanide ion ( $\text{Ln}^{3+}$ ) may inhibit certain enzymatic reactions involved in blood clotting requiring  $\text{Ca}^{2+}$  and especially impede the bioactivity of the blood coagulation factors and prothrombin. As a result, a longer activated partial thromboplastin time is observed from the La and Nd implanted samples due to these mechanisms.

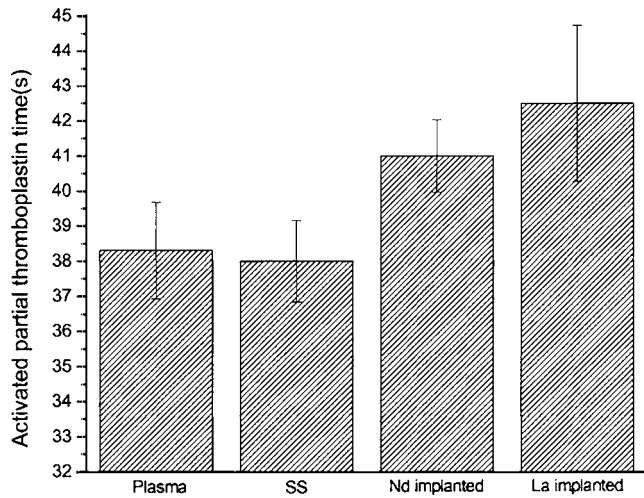


Fig. 6. Activated partial thromboplastin times of blood plasma, stainless steel, stainless steel implanted with La, and stainless steel implanted with Nd.

And more work is being performed to fathom the mechanisms in more detail.

#### IV. CONCLUSION

Stainless steel samples implanted with La and Nd form  $\text{La}_2\text{O}_3$  and  $\text{Nd}_2\text{O}_3$  oxide layers in the top 10–20 nm after exposure to air. The presence of the oxides dramatically improves the corrosion resistance of the implanted materials. Unlike other common elements, these rare earth elements also improve the biological properties of the materials. The activated partial thromboplastin time determined from the La and Nd implanted samples is prolonged and the results suggest that the antithrombogenic behavior of stainless steel implanted with La and Nd was enhanced compared with untreated stainless steel. Hence, rare earth element ion implantation can be used to improve the surface corrosion resistance and biomedical properties of 316 stainless steels.

#### ACKNOWLEDGEMENT

This work was supported by Hong Kong Research Grants Council (RGC) and National Science Foundation of Science (NSFC) Joint Research Project No. N\_CityU 101/03.

<sup>1</sup>C. H. Evans, *Biochemistry of the Lanthanides* (Plenum, New York, 1990), pp. 391 and 417.

<sup>2</sup>M. A. Jakupec, P. Unfried, and B. K. Keppler, *Rev. Physiol. Biochem. Pharmacol.* **153**, 101 (2005).

<sup>3</sup>J. Z. Gao, Q. J. Long, and Y. Tao, *J. Northwest Normal Univ., Natural*

*Science* **138**, 108 (2002).

<sup>4</sup>K. Przybylski, A. J. Farratt-Reed, and F. J. Yurek, *J. Electrochem. Soc.* **135**, 509 (1988).

<sup>5</sup>D. Q. Peng, X. D. Bai, and B. S. Chen, *Surf. Coat. Technol.* **190**, 440 (2005).

<sup>6</sup>M. A. Arenas, J. J. de Damborenea, A. Medrano, J. A. Garcia, and R. Rodriguez, *Surf. Coat. Technol.* **158**, 615 (2002).

<sup>7</sup>A. L. Rudd, C. B. Breslin, and F. Mansfeld, *Corros. Sci.* **42**, 275 (2000).

<sup>8</sup>P. Burroughs, A. Hamnett, A. F. Orchard, and G. Thornton, *J. Chem. Soc. Dalton Trans.* **1976**, 1686.

<sup>9</sup>V. Ashworth, D. Baxter, W. A. Grant, R. P. M. Procter, and T. C. Wellington, *Corros. Sci.* **16**, 775 (1976).

<sup>10</sup>J. Chen, J. R. Conrad, and R. A. Dodd, *J. Mater. Process. Technol.* **49**, 115 (1995).

<sup>11</sup>M. Iwaki, *Crit. Rev. Solid State Mater. Sci.* **15**, 473 (1989).

<sup>12</sup>M. V. Karimi, S. K. Sinha, D. C. Kothari, A. K. Khann, and A. K. Tyagi, *Surf. Coat. Technol.* **609**, 158 (2002).

<sup>13</sup>R. Leutenecker, G. Wagner, T. Louis, U. Gonser, L. Guzman, and A. Molinari, *Mater. Sci. Eng., A* **115**, 229 (1989).

<sup>14</sup>R. W. Y. Poon, J. P. Y. Ho, X. Y. Liu, C. Y. Chung, P. K. Chu, K. W. K. Yeung, W. W. Lu, and K. M. C. Cheung, *Mater. Sci. Eng., A* **390**, 444 (2005).

<sup>15</sup>Y. Sugizaki, T. Yasunaga, and H. Tomari, *Surf. Coat. Technol.* **83**, 167 (1996).

<sup>16</sup>W. Wang, J. H. Booske, C. Baum, C. Clothier, N. Zjaba, and L. Zhang, *Surf. Coat. Technol.* **111**, 97 (1999).

<sup>17</sup>K. A. Khan, F. Snyder, and L. M. Pechet, *J. Thromb. Thrombolysis* **6**, 159 (1998).

<sup>18</sup>D. A. Pawlak, M. Ito, M. Oku, K. Shimamura, and T. Fukuda, *J. Phys. Chem. B* **106**, 504 (2002).

<sup>19</sup>A. Galtayries *et al.*, *Surf. Interface Anal.* **27**, 941 (1999).

<sup>20</sup>D. Q. Peng, X. D. Bai, X. W. Chen, and Q. G. Zhou, *Surf. Coat. Technol.* **165**, 268 (2003).

<sup>21</sup>Q. H. Wu, M. L. Liu, and W. Jaegerman, *Mater. Lett.* **59**, 1480 (2005).

<sup>22</sup>Y. Uwamino, Y. Ishizuka, and H. Yamatera, *J. Electron Spectrosc. Relat. Phenom.* **34**, 69 (1984).

<sup>23</sup>K. Tabata, I. Matsumoto, and S. Kohiki, *J. Mater. Sci.* **22**, 1882 (1987).

<sup>24</sup>N. Gunasekaran, N. Bakshi, C. B. Alcock, and J. J. Carberry, *Solid State Ionics* **83**, 145 (1996).

<sup>25</sup>J. F. Moulder, W. G. Stickle, P. E. Sobol, and K. D. Bomben, *Handbook of X-Ray Photoelectron Spectroscopy* (Physical Electronics, MN, 1995), pp. 62 and 149.

<sup>26</sup>S. Kohiki, S. Hayashi, H. Adachi, S. Hatta, K. Setsune, and K. Wasa, *J. Phys. Soc. Jpn.* **41**, 39 (1989).

<sup>27</sup>E. Talik, M. Kruczek, H. Sakowska, Z. Ujma, M. Gała, and M. Neumann, *J. Alloys Compd.* **377**, 259 (2004).

<sup>28</sup>M. A. Arenas, J. J. de Damborenea, A. Medrano, J.-A. Garcia, and R. Rodriguez, *Surf. Coat. Technol.* **158**, 615 (2002).

<sup>29</sup>I. K. Kang, O. H. Kwon, and K. H. Byun, *J. Mater. Sci.* **7**, 135 (1996).

<sup>30</sup>Y. H. Feng, and X. X. Zheng, *J. Appl. Polym. Sci.* **74**, 2826 (1999).

<sup>31</sup>T. Funakoshi, K. Furushima, H. Shimada, and S. Kojima, *Biochem. Int.* **28**, 113 (1992).

<sup>32</sup>C. H. Evans, *Biochemistry of the Lanthanides* (Plenum, New York, 1990), pp. 24 and 25.

<sup>33</sup>B. C. Furie, K. G. Mann, and B. Furie, *J. Biol. Chem.* **251**, 3235 (1976).

<sup>34</sup>E. W. Davie, K. Fujikawa, and W. Kisiel, *Biochemistry* **30**, 10363 (1991).

<sup>35</sup>C. M. Heldebrant, R. J. Butkowski, S. P. Bajaj, and K. G. Mann, *J. Biol. Chem.* **248**, 7149 (1973).